# Extreme ultraviolet performance of a multilayer coated high density toroidal grating

Roger J. Thomas, Ritva A. M. Keski-Kuha, Werner M. Neupert, Charles E. Condor, and Jeffrey S. Gum

The performance of a multilayer coated diffraction grating has been evaluated at EUV wavelengths both in terms of absolute efficiency and spectral resolution. The application of a ten-layer Ir/Si multilayer coating to a 3600-lines/mm blazed toroidal replica grating produced a factor of 9 enhancement in peak efficiency near the design wavelength ~30 nm in first order, without degrading its excellent quasistigmatic spectral resolution. The measured EUV efficiency peaked at 3.3% and was improved over the full spectral range between 25 and 35 nm compared with the premultilayer replica which had a standard gold coating. In addition, the grating's spectral resolution of >5000 was maintained. *Key words:* EUV, multilayer, coating, grating.

## I. Introduction

The development of multilayer coatings with enhanced normal incidence reflectance allows us to take advantage of conventional normal incidence mirror technology for instruments that operate at x-ray or EUV wavelengths. An extensive amount of work has already been done on applying multilayer coatings to mirrors both for laboratory applications and for astronomical applications in sounding rocket experiments.[1–10] It would also be desirable to apply this technology to diffraction gratings to provide enhanced efficiency for normal incidence spectrographs in wavelength regions where only glancing incidence designs have provided acceptable throughput in the past.

The application of multilayer coatings to diffraction gratings for use in the spectral region below 20 nm has been studied by several investigators, resulting in multilayer coatings that provide gratings with enhanced efficiency over a narrow bandpass.[11–15] Enhancement has also been demonstrated in the 30-nm spectral region for a sinusoidal grating.[3] We discuss in this paper the application of a multilayer coating to a large, concave, aspheric diffraction grating, a 3600-lines/mm toroidal blazed replica, designed for operation in the 30-nm spectral region in first order.

Preliminary results of this work were reported in Ref. 16. An initial version of this paper was also presented at the SPIE Conference on Multilayer Coated Optics in San Diego, July 1990, and appears in the Proceedings of that meeting.[17]

The authors are with NASA Goddard Space Flight Center, Greenbelt, Maryland 20771.

Received 18 September 1990.

## II. Grating Characteristics

The grating coated for this study was originally developed for the solar EUV rocket telescope and spectrograph (SERTS).[18] The optical concept of that instrument uses a grazing incidence Wolter type-2 telescope to feed a quasistigmatic spectrograph, in which the toroidal grating operating near normal incidence acts to reimage a spectrally dispersed version of the solar image falling onto its entrance aperture. The measured optical parameters for the SERTS master grating are shown in Table I.

The high quality concave toroidal shape of the master grating's optical surface was polished directly into the Zerodur substrate by Capricorn Optical Corp. In addition to standard comparisons against a spherical test plate, measurements of the toroid's two radii of curvature, and of the surface figure error, were made optically in visible light during this polishing procedure with a laser unequal path interferometer (Fig. 1). The measurement takes advantage of the fact that such toroidal surfaces produce stigmatic imaging in zero order when operated in a special configuration that has a known relationship to the surface parameters. In this configuration, the laser source is focused through a point to illuminate the toroidal grating, which produces an image of the source point in zero order. A precision polished sphere centered on the grating image point then sends the beam back through the optical train, so that the interferometer can compare the outgoing and returning wavefronts. After the

Table I. SERTS Grating Parameters

| | |
|---|---|
| Substrate material | Zerodur |
| Dimensions | 95 × 85 mm |
| Optical surface shape | Toroid (prolate spheroid) |
| Dispersion radius ($R_t$) | 1209.67 mm |
| Cross radius ($R_s$) | 1200.02 mm |
| Radius ratio ($R_s/R_t$) | 0.9920 |
| Surface figure error | 40 nm (peak to valley) |
| Ruling frequency | 3600 lines/mm |
| Ruling width | 65 mm |
| Ruling length | 80 mm |
| Grating blaze | 2.8° (tripartite) |
| Coating | Gold |

system is adjusted to minimize the measured wavefront differences, the distance from the source to image point ($2 \times L$) and the perpendicular distance from the source–image line to the grating vertex ($D$) are related to the grating blank's two radii of curvature as follows:

$$R_s = D, \qquad R_t = (L^2 + D^2)/D. \tag{1}$$

The residual wavefront differences are then a direct measurement of the figure error in the toroidal surface in units of the source laser wavelength. This procedure is particularly sensitive in that the test beam is modulated twice by a given point on the grating surface for each measurement.

The master was ruled and gold coated at Hyperfine, Inc., which also made several replicas from it by means of a convex toroidal submaster and concave toroidal replica blanks. The gratings were then tested for EUV efficiency at the Synchrotron Ultraviolet Radiation Facility (SURF-II) of the National Institute of Standards & Technology (NIST) in Gaithersburg, Maryland. Their spectral resolutions were also measured in a spectrograph test chamber developed for that purpose by the Solar Physics Branch at GSFC. These measurements were used to select the best replica for flight on the SERTS experiment. The grating chosen for the multilayer study described here was one of the flight spare replicas from this group. It had no special processing to prepare it for the multilayer coating procedure.

## III. Coating Process

The coating selected for the grating was a ten-layer Ir/Si multilayer optimized for 30.4 nm at a normal incidence angle of 15°, with a theoretical peak reflectance of 21% at that angle. Starting from the substrate, the design thicknesses of the layers (in nanometers) are as follows: Si, 10.2; Ir, 8.9; Si, 11.0; Ir, 7.0; Si, 11.6; Ir, 6.0; Si, 11.9; Ir, 5.5; Si, 12.1; and Ir, 5.2. The optical constants used in the calculations are reported in Refs. 19 and 20 for Ir films and Refs. 21–23 for Si films. The multilayer coating was deposited directly onto the gold base coating using e-beam evaporation in a 2-m diam evaporator[24] at GSFC. Four 5- × 5-cm microscope slides were mounted next to the grating. The grating and the microscope slides were located 83 cm above the source, and the center of the grating was offset 9 cm from the center of the source. Based on distribution studies, the layer thickness uniformity across the grating was ~2%.

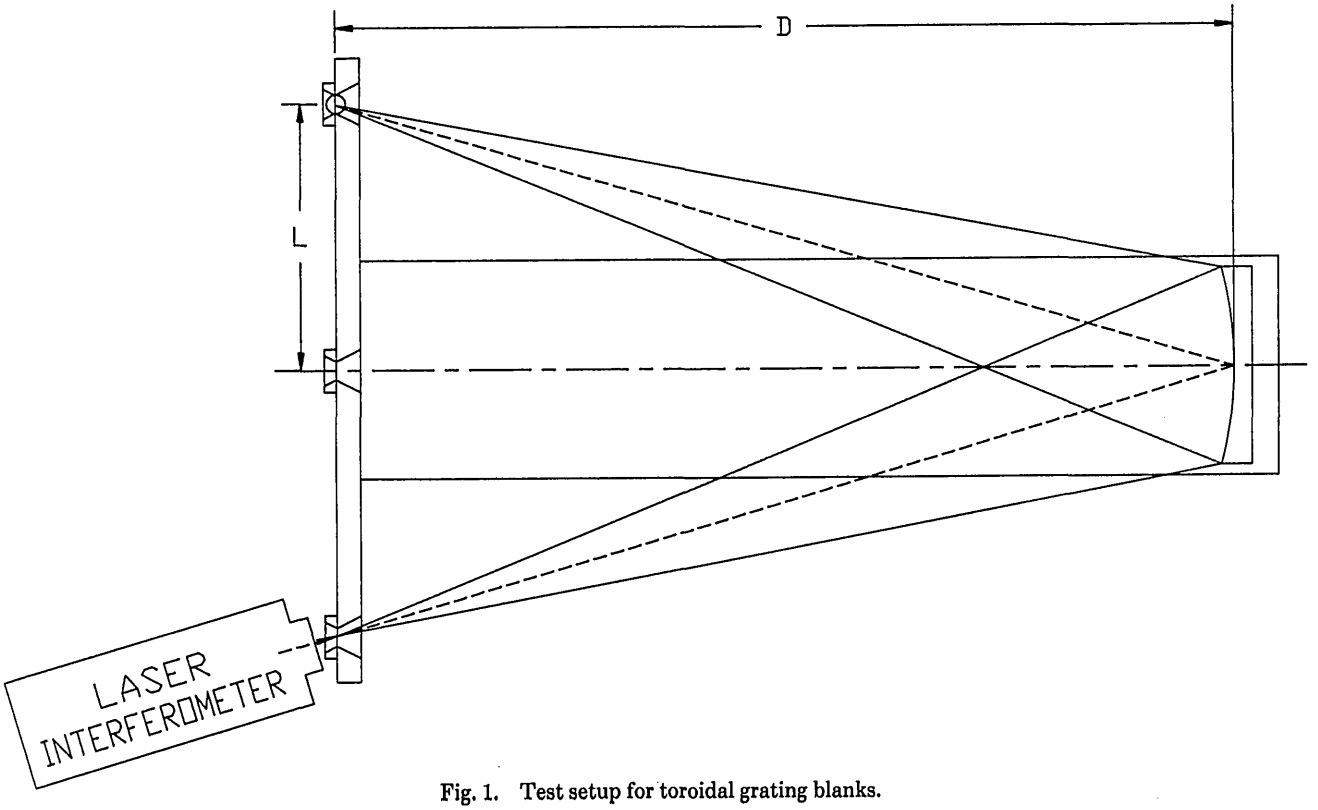


Fig. 1. Test setup for toroidal grating blanks.

The EUV reflectances of the microscope slide coatings were measured using a reflectometer–monochromator system described elsewhere.[25] At a 15° angle of incidence, the 30.4-nm reflectance varied from 15.0 to 15.3% on the four microscope slides with the slide located farthest away from the source having the highest reflectance. The 30.4-nm reflectance of that coating increased to 16.1% at a 12° angle of incidence, which, because of instrument limitations, is the smallest angle that can be measured. Such behavior indicates that the peak reflectance of the actual coating occurs somewhat short of the design wavelength.

## IV. Grating Test Procedure and Results

### A. Efficiency

Absolute EUV efficiencies were measured at the SURF-II operated by the Center for Radiation Research, National Measurement Laboratory, at the NIST. This facility provides a well-characterized national radiometric standard throughout the XUV spectral range, with an overall accuracy of ~2% as determined by intercomparison with a variety of transfer standards. The radiation produced is a highly plane polarized XUV continuum that emerges in a narrow, approximately collimated beam. Of the several beam lines available, our grating measurements were carried out on beam line 2, which has been designated as a spectrometer calibration beam line and is under the partial sponsorship of NASA. The measurements reported here were made at the first of the two calibration stations on beam line 2, located 11.5 m from the storage ring tangent point. It has provisions for precision controlled two-axes translation and rotation, permitting accurate angular alignment and subaperture mapping over the grating's ruled area.

The principal features of our grating calibration chamber are shown in Fig. 2. The chamber is first aligned to the synchrotron beam in visible light by a reference mirror attached to its rear wall. Then the test grating is installed at its normal operating angle of 7.0° and the chamber is evacuated. When the SURF-II beam is allowed to illuminate the grating, its alignment can be verified by the location of the visible zero-order spot seen on the side viewing port window. Pitch scans can also be performed to assure that the detector is properly centered relative to the dispersion plane. The diffracted EUV beam falls onto an exit slit 2.0 mm wide by 9.0 mm long placed in front of a windowless photodiode whose EUV response vs wavelength has been independently calibrated by NIST personnel. The output of the photodiode is determined by an electrometer, which is itself independently recalibrated as needed.

The exit slit and photodiode are mounted on an arm that pivots about an axis passing through the grating's vertex and perpendicular to its dispersion plane. The position of the arm is controlled from outside the vacuum chamber through a mechanical linkage and is measured by reading an odometer type dial on the arm gearing. This allows tests of the grating efficiency over the full wavelength range from ~20 to 60 nm. The conversion between arm readings and a wavelength scale was determined by geometric considerations and is checked periodically by carrying out measurement runs that include appropriate edge filters. For that purpose, thin filters of Ge and Sn/Ge are occasionally placed in the beam to introduce discontinuities at known wavelengths in the otherwise smoothly varying EUV continuum distribution, thus providing identifiable wavelength fiducials. We estimate that the accuracy of the resulting wavelength scale is about ±0.5 nm.

The size of the SURF-II beam is defined by a 13-mm circular aperture that is 10.538 m from the synchrotron tangent point. The grating being tested is located 11.922 m from the tangent point, and so the instantaneously illuminated area is 14.7 mm in diameter. Dur-

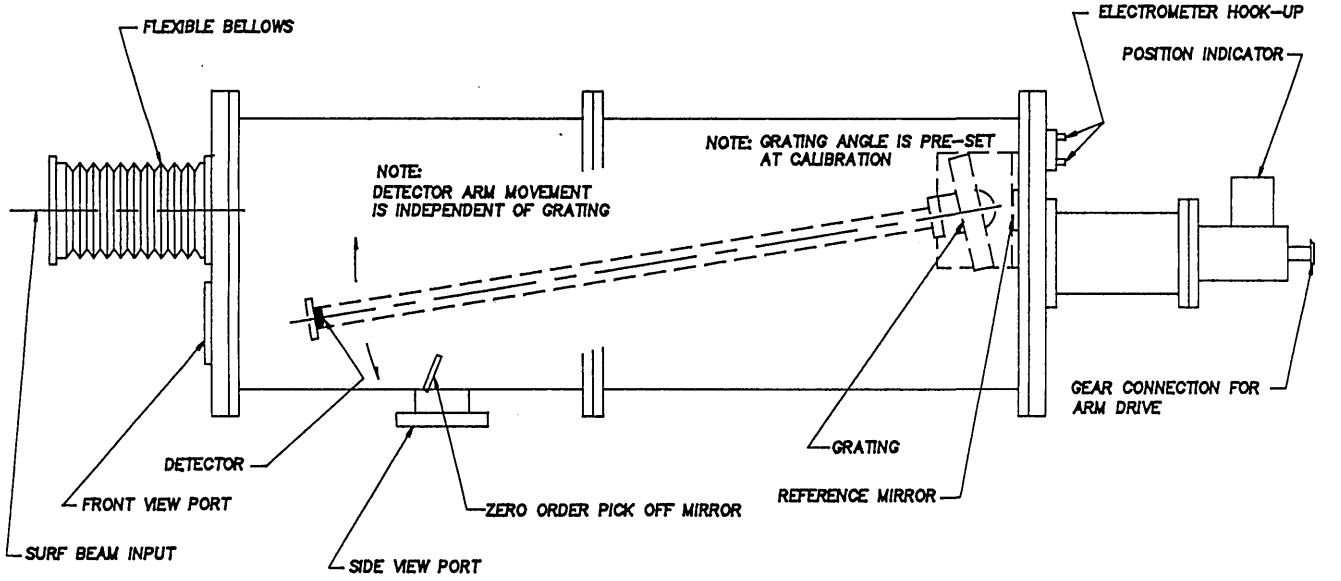


Fig. 2. NIST grating evaluation chamber.

ing a measurement run, the chamber is translated in a rectangular pattern of 17.7-mm increments so that a total of nine subaperture surface positions is mapped. Because of length limitations, the distance from the grating vertex to the exit slit is only 55 cm instead of the true focal distance of 63.67 cm for the SURF test configuration as determined by ray trace calculations. Thus, the size of a diffracted spot of a given wavelength at the exit slit is

$$S = 14.7 \times (63.67 - 55)/63.67 = 2.0 \text{ mm}, \quad (2)$$

which sets the lower limit on the useful width of the exit slit. Since the spectral dispersion at that distance is 0.505 nm/mm, the FWHM of the detector's response for each position setting is 1.01 nm.

Along with readings of the dial indicator for the detector arm position and electrometer values for the photodiode output, the synchrotron beam current is recorded at the beginning and end of the wavelength scans for each of the nine grating locations illuminated. For the beam conditions on that day, this allows a determination of the exact incident flux as a function of wavelength from tables supplied by the SURF-II operators. It should be noted that the synchrotron radiation in our wavelength range is ~97% polarized in the plane perpendicular to the grating rulings, and so all the efficiency results reported here refer only to that situation. (We have not yet made any measurements in the orthogonal orientation, although we have now modified our calibration chamber to allow us to make such measurements in the future.)

A SERTS flight spare replica grating, serial number 605-12-1, with a standard gold coating was measured at the NIST in this way on 26 Oct. 1989. The grating was then taken to GSFC and overcoated with a ten-layer Ir/Si multilayer optimized for 30.4 nm, as described above. It was then returned to the NIST and remeasured in the grating evaluation chamber on 7 Nov. 1989.

Since reporting our initial results in Refs. 16 and 17, we have refined the calibration analysis, especially in terms of its wavelength scale, resulting in slight changes to the calculation of efficiency enhancement ratios compared to those reported earlier.

Incorporating these new calibrations, the absolute grating efficiency averaged over each of the nine measured positions before and after application of the multilayer coating is shown in Fig. 3 along with a normalized curve of the calculated theoretical reflectance for the multilayer design itself. Here, the theoretical curve was calculated by assuming 100% transverse magnetic polarization at a normal incidence angle of 7.0°, and then averaging over the 1-nm bandpass of the photodiode detector. The ratio of efficiencies combined from all positional measurements is given in Fig. 4. Below 25 nm, the individual efficiencies were low enough to cause considerable scatter in the measured ratio values, but at longer wavelengths the ratio seems to be remarkably uniform over the nine different locations on the grating.

The revised analysis shows that the multilayer coating produced a peak absolute efficiency of 3.3% in first order at 31.2 nm. This represents the highest efficiency at that wavelength yet reported for a high resolution grating operating at near normal incidence, to our knowledge. The greatest improvement occurred at 29.7 nm, where the grating's first-order efficiency increased from 0.30 to 2.8%, more than a factor of 9 above that of the standard gold coating. The multilayer coating provided some enhancement over the entire 10-nm band from 25 to 35 nm, and at least a factor of 5 enhancement over the 6.3-nm band from 26.2 to 32.5 nm. In fact, the measurements suggest that efficiency was even enhanced over the short wavelength band from 20 to 25 nm, although the individual values were so low that resulting ratios are uncertain there. Above 25 nm where response readings were sufficiently high, the uncertainty of individual absolute efficiency measurements is ~50%, primarily because of a possibility that the photodiode may have lost sensitivity since the time it was last calibrated. Such a loss in photodiode sensitivity would mean that the absolute grating effi-

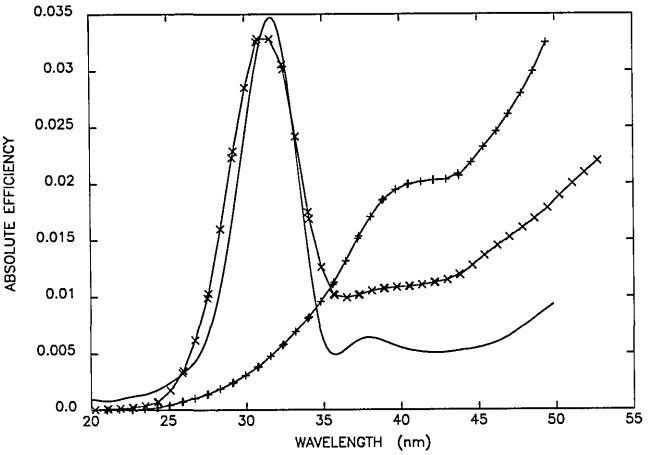


Fig. 3. Absolute EUV efficiency of the SERTS test grating before (+) and after (×) multilayer coating. For comparison, the solid curve is the calculated theoretical reflectance of the design multilayer itself, scaled by a normalization factor of 0.14.

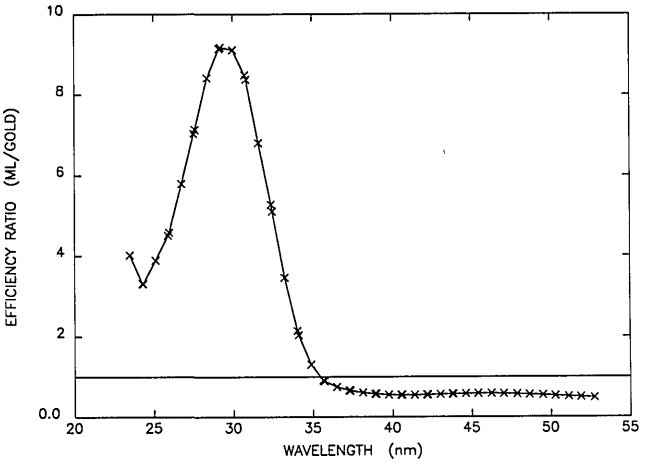


Fig. 4. Enhancement in first-order EUV efficiency for the SERTS multilayer coated grating.

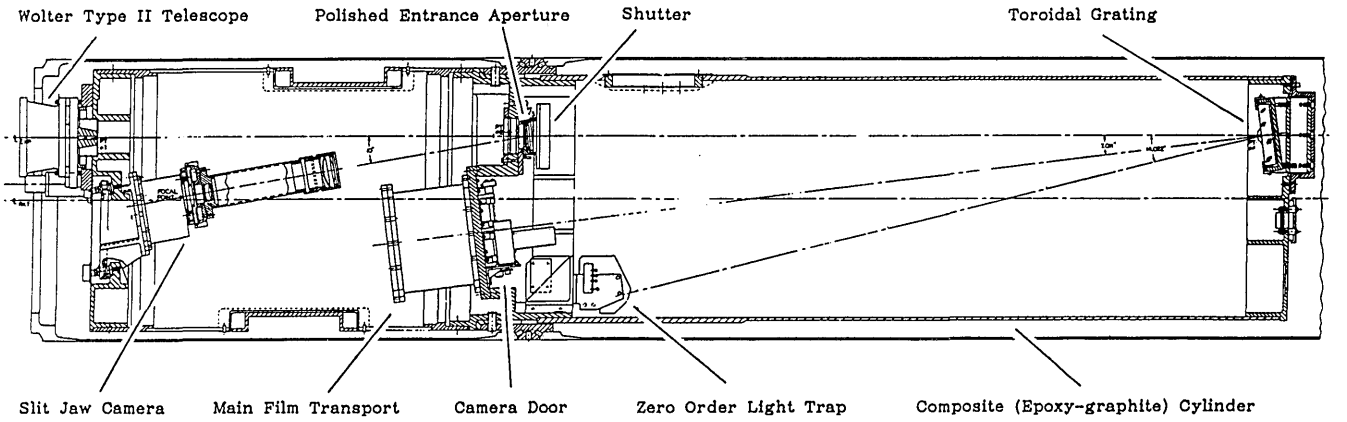

Fig. 5. Solar EUV Rocket Telescope and Spectrograph.

ciencies are actually even higher than we have reported here, while it would have no effect on the enhancement ratios shown in Fig. 4. The efficiency ratio values above 25 nm should be accurate to <10%, since their only significant source of error is uncertainty in comparing the wavelength scales of the before and after measurements.

Using a constant normalization factor of 14% (presumably resulting in large part from the grating groove efficiency), the theoretically predicted reflectance curve agrees quite well with the measured absolute efficiency of the multilayer grating, as shown in Fig. 3. The multilayer grating efficiency does seem to peak at a wavelength ~0.5 nm less than that for the design curve, which is consistent with the microscope slide test results mentioned in Sec. III. However, it should be noted that this apparent shift is also about equivalent to uncertainties in the measurement's absolute wavelength scale. One definite difference is that the design FWHM bandwidth of 4.5 nm is somewhat narrower than the actual measured value of 5.5 nm.

In any case, these bandwidths for multilayer coated gratings are well matched to spectrographic instruments that use 2-D array detectors such as EUV sensitive CCDs, whose active dimensions can be as large as 1 or 2 cm. With a number of pixels of the order of 1000, such a system could provide a spectral resolution of ~5000 over a bandpass of >40 nm at EUV wavelengths with high sensitivity, if the multilayer coating itself did not significantly degrade the spectral performance of the toroidal grating.

### B. Spectral Resolution

To investigate that possibility, we made before and after measurements of the multilayer grating's spectral resolution in the SERTS spectrograph test chamber at GSFC. This facility allows the spectrograph section of the SERTS rocket instrument itself (shown in Fig. 5) to be attached to a vacuum system provided with a hollow cathode gas flow EUV light source. The light source uses a combination of helium and neon gases to produce a large number of spectral lines throughout the EUV wavelength range of interest. Radiation from the source lamp is concentrated on the spectrograph entrance aperture by means of a grazing incidence ellipsoidal mirror to increase the system's speed. The resultant images are recorded on Kodak special film, Type 101-07, which has been specifically developed for sensitivity in the EUV. Since the spectrograph's entrance aperture, aluminum filter, toroidal grating, and film camera can all be flight units, this arrangement permits the final alignment and focus adjustments to be made on the SERTS optical components, as well as providing the preflight and postflight instrumental performance parameters directly in the EUV wavelengths of interest.

For the tests reported here, the original resolution measurements were made on the toroidal grating that was used in the two most recent flights of the SERTS rocket experiment, as a part of their preflight and postflight calibrations. At that time, the grating selected for flight (serial number 605-10-1) demonstrated a spectral resolution similar to its replica mate (605-12-1). (Grating 605-10-1 was selected for flight primarily on the basis of its superior efficiency, measured to be 0.80% at 30.4 nm.) After the flight spare grating (605-12-1) was coated with the ten-layer Ir/Si multilayer, and after its EUV reflectance was remeasured at the NIST, it was substituted for the SERTS-3 flight grating in the spectrograph test chamber and a total of seven EUV exposures of various durations were made in a single configuration run. It should be noted that there was no attempt to fine tune the multilayer grating's alignment or EUV focus, and therefore the results may be somewhat less than optimized.

The spectrograph entrance aperture is made up of two parts, a narrow slit near the instrument's imaging axis, and a wider slot or lobe on each end of the slit, as shown schematically in Fig. 6. The quasistigmatic operation of the toroidal grating acts to produce spectrally dispersed images of this entrance aperture along the spectrograph's focal surface in the EUV emission lines of the illuminating source, thus providing both spectral and spatial information at wavelengths from ~24 to 45 nm. The present design parameters of the SERTS spectrograph, and therefore of the spectrograph test chamber, are given in Table II. Although this design is strictly stigmatic at only two specific

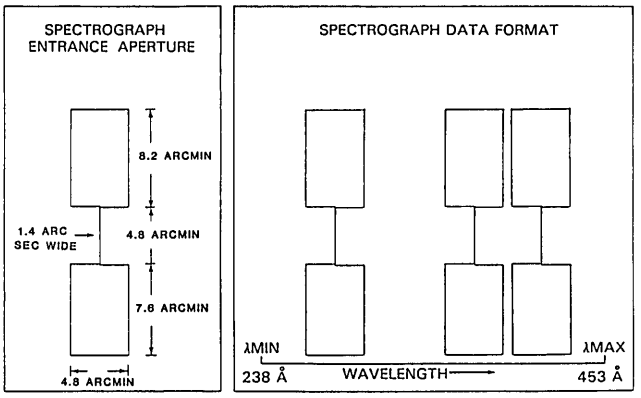


Fig. 6. Layout of the SERTS spectrograph entrance aperture.

**Table II. SERTS Spectrograph Parameters**

| | |
|---|---|
| Grating dispersion radius ($R_t$) | 1209.67 mm |
| Grating cross radius ($R_s$) | 1200.02 mm |
| Grating ruling frequency | 3600 lines/mm |
| Grating operating angle | 7.01° |
| Object distance | 1150 mm |
| Average image distance | 1265 mm |
| Spatial image magnification | 1.10 |
| Spectral dispersion | 0.22 nm/mm |
| Physical length of spectrum | 97.3 mm |
| Spectral range | 23.5–44.9 nm |
| Narrow slit width | 13-$\mu$m (SERTS-2), 15-$\mu$m (SERTS-3) |
| Narrow slit length | 1.7-mm (SERTS-2), 3.0-mm (SERTS-3) |
| Lobe slot width | 0.5-mm (SERTS-2), 3.0-mm (SERTS-3) |
| Lobe slot length | 4.5-mm (SERTS-2), 5.0-mm (SERTS-3) |

wavelengths, the system's sagittal and tangential focuses are sufficiently close over the full spectral range that the resultant spot sizes are determined almost entirely by factors other than limitations in theoretical performance.

Figure 7 shows a representative postflight EUV Ne–He spectrum taken on 1 Nov. 1989 with the SERTS-3 replica grating (605-10-1) and entrance aperture, as compared with one taken on 4 Jan. 1990 in the identical spectrograph chamber but with the backup replica grating (605-12-1) and its multilayer coating. The enhanced strength of the recorded lines ~30 nm can be seen in the multilayer spectrum, although this is at least partially affected by differences in source intensity and exposure time between these two photographs. The two spectra are shifted relative to one another by 0.77-nm wavelength, so that the strong line at the far right of the upper spectrum falls outside the observed range of the lower one. This suggests that the operating angle of the multilayer grating was tilted by ~5 min of arc relative to the SERTS flight grating. Ray trace calculations indicate that, without a corresponding focus correction, such a tilt could cause the theoretical (zero slit) spot diameter in the spectral dimension to increase from the average aligned value of 0.4 pm (physical size of 1.9 $\mu$m) to as much as 1.5 pm (physical size of 6.9 $\mu$m) in the misaligned case.

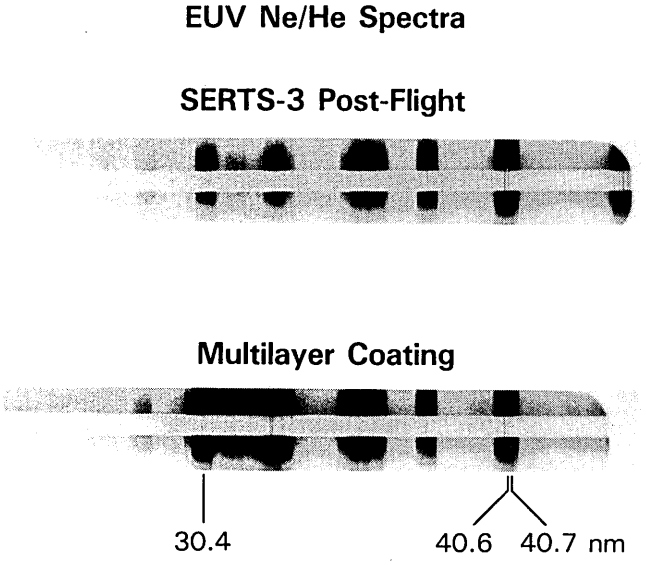


Fig. 7. EUV Ne–He spectra produced with a gold coated grating (top) and with a multilayer coated grating (bottom).

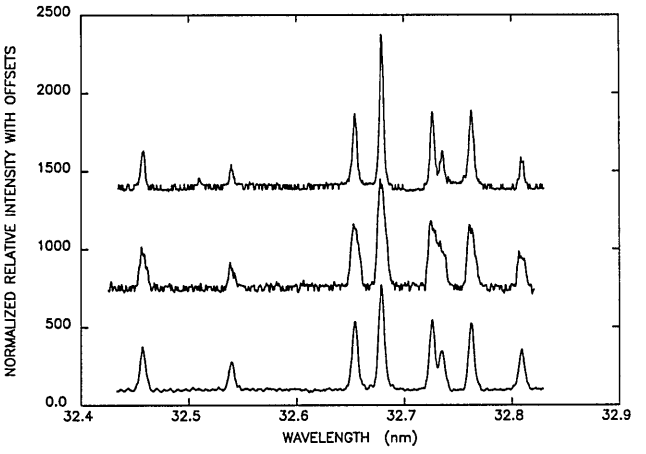


Fig. 8. Microdensitometer traces of EUV Ne II spectra produced with a gold coated grating (top and middle) and with a multilayer coated grating (bottom). The top curve is from SERTS-2 preflight tests; the middle one is from SERTS-3 preflight tests.

Spectral traces over a number of EUV Ne II lines are shown in Fig. 8, which compares the resolution of the

**Table III. Measured Spectral Performance**

| Grating | Imaged slit width ($\mu$m) Spectrom. | Imaged slit width ($\mu$m) Microdens. | Averaged EUV line FWHM Linear ($\mu$m) | Averaged EUV line FWHM Spectral (pm) | Resolution at 32 nm |
|---|---|---|---|---|---|
| 605-10-1 SERTS-2 | 14.3 | 2.5 | 21 ± 2 | 4.7 ± 0.4 | 6800 ± 600 |
| 605-10-1 SERTS-3 | 16.5 | 3.3 | 36 ± 2 | 8.0 ± 0.5 | 4000 ± 300 |
| 605-12-1 Multilayer | 16.5 | 2.5 | 27 ± 1 | 6.0 ± 0.1 | 5300 ± 100 |

multilayer coated grating (605-12-1) with the measurements made prior to the SERTS-2 and SERTS-3 rocket flights using grating 605-10-1. Clearly, the excellent spectral imaging properties of the grating have not been degraded by the multilayer coating or by the process of applying it. The average linewidths (FWHM) measured for the five strongest unblended lines seen in Fig. 8 (at 32.46, 32.65, 32.68, 32.76, and 32.81 nm) are given in Table III. The small differences are well within the expected variations resulting from errors in focusing or alignment, or from differences in the widths of the various slits used in the measurements.

## V. Conclusions

Summarizing, the application of a multilayer coating to a large, high density, aspheric diffraction grating replica has produced a significant enhancement in first-order efficiency over more than a 6-nm spectral band at wavelengths ~30 nm. This implies that a considerable improvement in throughput can be achieved in EUV instruments like SERTS that use gratings at normal incidence. The studies carried out to compare the spectral performance for the SERTS flight spare grating after depositing the multilayer coating demonstrate that the grating suffered no loss in its excellent spectral resolution due to the coating process. An investigation of the long-term stability of this multilayer coated grating is planned for the future.

This work has been supported under NASA RTOP grants 170-38-51-10 and 879-11-38 from the Solar Physics Office of NASA's Space Physics Division.

## References

1. E. Spiller, "Reflective Multilayer Coatings for the Far UV Region," Appl. Opt. **15**, 2333–2338 (1976).
2. J. H. Underwood and T. W. Barbee, Jr., "Layered Synthetic Microstructures as Bragg Diffractors for X Rays and Extreme Ultraviolet: Theory and Predicted Performance," Appl. Opt. **20**, 3027–3034 (1981).
3. R. A. M. Keski-Kuha, "Layered Synthetic Microstructure Technology Considerations for the Extreme Ultraviolet," Appl. Opt. **23**, 3534–3537 (1984).
4. T. W. Barbee, Jr., S. Mrowka, and M. C. Hettrick, "Molybdenum–Silicon Multilayer Mirrors for the Extreme Ultraviolet," Appl. Opt. **24**, 883–886 (1985).
5. J. F. Meekins, R. G. Cruddace, and H. Gursky, "Optimization of Layered Synthetic Microstructures for Narrowband Reflectivity at Soft X-Ray and EUV Wavelengths," Appl. Opt. **25**, 2757–2763 (1986).
6. J. F. Lindblom, A. B. C. Walker, Jr., R. B. Hoover, T. W. Barbee, Jr., R. A. van Patten, and J. P. Gill, "Soft X-Ray/Extreme Ultraviolet Images of the Solar Atmosphere with Normal Incidence Multilayer Optics," Proc. Soc. Photo-Opt. Instrum. Eng. **982**, 316–324 (1988).
7. B. M. Haisch, T. E. Whittmore, E. G. Joki, W. J. Brookover, and G. J. Rottman, "A Multilayer X-Ray Mirror for Solar Photometric Imaging Flown on a Sounding Rocket," Proc. Soc. Photo-Opt. Instrum. Eng. **982**, 38–45 (1988).
8. R. C. Catura and L. Golub, "XUV Multilayered Optics for Astrophysics," Rev. Phys. Appl. **23**, 1741–1746 (1988).
9. A. B. C. Walker, Jr., T. W. Barbee, Jr., R. B. Hoover, and J. F. Lindblom, "Soft X-Ray Images of the Solar Corona with a Normal Incidence Cassegrain Multilayer Telescope," Science **241**, 1781–1787 (1989).
10. L. Golub, M. Herant, K. Kalata, I. Lovas, G. Nystrom, F. Pardo, E. Spiller, and J. Wilczynski, "Sub-Arcsecond Observations of the Solar X-ray Corona," Nature London **344**, 842–844 (1990).
11. J. C. Rife, W. R. Hunter, T. W. Barbee, Jr., and R. C. Cruddace, "Multilayer-Coated Blazed Grating Performance in the Soft X-Ray Region," Appl. Opt. **28**, 2984–2986 (1989).
12. T. W. Barbee, Jr., "Combined Microstructure X-Ray Optics," Rev. Sci. Instrum. **60**, 1588–1595 (1989).
13. J. C. Rife, T. W. Barbee, Jr., W. R. Hunter, and R. G. Cruddace, "Performance of a Tungsten/Carbon Multilayer-Coated Blazed Grating from 150 to 1700 eV," Phys. Scr. **41**, 418–421 (1990).
14. R. G. Cruddace, T. W. Barbee, Jr., J. C. Rife, and W. R. Hunter, "Measurements of the Normal-Incidence X-Ray Reflectance of a Molybdenum-Silicon Multilayer on a 200-l/mm Grating," Phys. Scr. **41**, 396–399 (1990).
15. J. V. Bixler, T. W. Barbee, Jr., and D. D. Dietrich, "Performance of Multilayer Coated Gratings in the Extreme Ultraviolet," Proc. Soc. Photo-Opt. Instrum. Eng. **1160**, 648–654 (1989).
16. R. A. M. Keski-Kuha, R. J. Thomas, J. S. Gum, and C. E. Condor, "Performance of Multilayer Coated Diffraction Gratings in the EUV," Appl. Opt. **29**, 4529–4531 (1990).
17. R. A. M. Keski-Kuha, R. J. Thomas, W. M. Neupert, C. E. Condor, and J. S. Gum, "EUV Performance of a Multilayer Coated High-Density Toroidal Grating," Proc. Soc. Photo-Opt. Instrum. Eng. **1343**, 566–575 (1990).
18. W. M. Neupert, G. L. Epstein, R. J. Thomas, and U. Feldman, "A Solar Ultraviolet Telescope and Spectrograph for Shuttle/Spacelab," Space Sci. Rev. **29**, 425–429 (1981).
19. G. Hass, G. F. Jacobus, and W. R. Hunter, "Optical Properties of Evaporated Iridium Films in the Vacuum Ultraviolet from 500 Å to 2000 Å," J. Opt. Soc. Am. **57**, 758–762 (1967).
20. J. F. Osantowski, NASA Goddard Space Flight Center; private communication.
21. W. R. Hunter, "Observation of Absorption Edges in the EUV by Transmittance Measurements through Thin Unbacked Metal Films," in *Optical Properties and Electronic Structure of Metals and Alloys*, F. Abeles, Ed. (North-Holland, Amsterdam, 1966), p. 136–146.
22. W. R. Hunter, "On the Optical Constants of Metals at Wavelengths Shorter than their Critical Wavelength," J. Phys. Paris **25**, 154–160 (1964).
23. W. R. Hunter, Sachs-Freeman Associates; private communication.
24. A. P. Bradford, G. Hass, J. F. Osantowski, and A. R. Toft, "Preparation of Mirror Coatings for the Vacuum Ultraviolet in a 2-m Evaporator," Appl. Opt. **8**, 1183–1189 (1969).
25. J. F. Osantowski, "Reflectance and Optical Constants for Cer-Vit from 250 to 1050 Å," J. Opt. Soc. Am. **64**, 834–838 (1974).